# Progenitors of Secondary Crest Myofibroblasts Are Developmentally Committed in Early Lung Mesoderm

CHANGGONG LI,[a] MIN LI,[a] SHA LI,[a] YIMING XING,[b] CHANG–YO YANG,[a] AIMIN LI,[a] ZEA BOROK,[c] STIJN DE LANGHE,[d,e] PARVIZ MINOO[a]

[a]Division of Newborn Medicine, Department of Pediatrics, Los Angeles County+University of Southern California Medical Center and Childrens Hospital Los Angeles and [c]Will Rogers Institute Pulmonary Research Center, Division of Pulmonary, Critical Care and Sleep Medicine, Department of Medicine, University of Southern California, Keck School of Medicine of USC, Los Angeles, California, USA; [b]The State Key Laboratory for Agro-Biotechnology, China Agriculture University, Beijing, People's Republic of China; [d]Division of Cell Biology, Department of Pediatrics, National Jewish Health, Denver, Colorado, USA; [e]Department of Cellular & Developmental Biology, School of Medicine, University of Colorado, Aurora, Colorado, USA

Correspondence: Parviz Minoo, PhD, Department of Pediatrics, LA County+ USC Medical Center, University of Southern California, Keck School of Medicine, Los Angeles, California 90033, USA. Telephone: 323-226-4340; Fax: 323-226-5049; E-mail: minoo@usc.edu

## ABSTRACT

Development of the mammalian lung is predicated on cross-communications between two highly interactive tissues, the endodermally derived epithelium and the mesodermally derived pulmonary mesenchyme. While much attention has been paid for the lung epithelium, the pulmonary mesenchyme, partly due to lack of specific tractable markers remains under-investigated. The lung mesenchyme is derived from the lateral plate mesoderm and is the principal recipient of Hedgehog (Hh) signaling, a morphogenetic network that regulates multiple aspects of embryonic development. Using the Hh-responsive *Gli1-cre*[ERT2] mouse line, we identified the mesodermal targets of Hh signaling at various time points during embryonic and postnatal lung development. Cell lineage analysis showed these cells serve as progenitors to contribute to multiple lineages of mesodermally derived differentiated cell types that include parenchymal or interstitial myofibroblasts, peribronchial and perivascular smooth muscle as well as rare populations of cells within the mesothelium. Most importantly, *Gli1-cre*[ERT2] identified the progenitors of secondary crest myofibroblasts, a hitherto intractable cell type that plays a key role in alveolar formation, a vital process about which little is currently known. Transcriptome analysis of Hh-targeted progenitor cells transitioning from the pseudoglandular to the saccular phase of lung development revealed important modulations of key signaling pathways. Among these, there was significant downregulation of canonical WNT signaling. Ectopic stabilization of β-catenin via inactivation of *Apc* by *Gli1-cre*[ERT2] expanded the Hh-targeted progenitor pools, which caused the formation of fibroblastic masses within the lung parenchyma. The *Gli1-cre*[ERT2] mouse line represents a novel tool in the analysis of mesenchymal cell biology and alveolar formation during lung development. STEM CELLS 2015;33:999–1012

## INTRODUCTION

Development of vertebrate organs is initiated by specification of a primordium within the early embryo and usually requires contributions from more than one germ layer. Ontogeny and development of the mammalian lung is no exception and requires contributions from at least two highly interactive embryonic tissues, the endodermally derived epithelium and the mesodermally derived pulmonary mesenchyme. Epithelial-mesenchymal interactions are centerpiece in both structural development of the lung as well as differentiation of its many highly specialized cell types.

While the last two decades have witnessed extensive analysis of the lung epithelium, the pulmonary mesoderm, partly due to lack of specific markers has been less tractable. The pulmonary mesenchyme is derived from the lateral plate mesoderm, which forms in the early embryo subsequent to gastrulation. One of the earliest mesodermal cell types to differentiate in the embryonic lung is distinguished by ACTA2 (alpha smooth muscle actin) expression. In the adult lung, the ACTA2-expressing lineages can be viewed as belonging to two large classes of mesodermally derived cell populations; smooth muscle cells and myofibroblasts. As early as embryonic day E11.5, ACTA2-expressing smooth muscle cells are found as distinct cell layers around the nascent airways and the mainstem bronchi that are formed by the first endodermal bifurcation. As development of the airways proceeds in a proximo-distal direction, the ACTA2-expressing smooth muscle lineage contributes to peribronchial and perivascular smooth muscle fibers (PBSM and PVSM, respectively) and possibly cells known as pericytes. Abnormalities in these structures have profound consequence on normal airway and vascular function and lead to diseases such as asthma and pulmonary hypertension.

The lung mesoderm also serves as the source of interstitial myofibroblasts (IMF), the contractile fibroblasts that express ACTA2. During early lung development (before saccular stage), progenitors of IMFs are scattered in the parenchyma of the lung. In these cells, ACTA2 is undetectable or absent, and no marker has been reported to distinguish them from other fibroblast progenitors. However, platelet-derived growth factor receptor alpha (PDGFα) was reported as a marker for IMF progenitors in saccular lungs [1, 2]. In the adult lung, IMFs appear as ACTA2$^{pos}$ cells embedded in the alveolar parenchyma but in much reduced numbers [3]. The function of IMF in the adult lung remains entirely unknown but the IMFs in the perinatal lung are the source of alveolar or secondary crest myofibroblasts (SCMFs). SCMFs are located at the tip of secondary crest structures during the saccular and alveolar phases of lung development. SCMFs have remained a highly intractable, elusive cell type, and there is urgent need to gain a better understanding of their biology. SCMFs play a key role in alveolar formation. In human pre-term neonates, interruption in alveogenesis underlies the pathogenesis of the chronic lung disease known as bronchopulmonary dysplasia (BPD). In adults, destruction of alveoli is a hallmark of emphysema and chronic obstructive pulmonary disease (COPD). Both the neonatal and adult manifestations of alveolar defects are highly morbid and can be lethal.

During embryonic development, the lung mesenchyme is the principal recipient of Hedgehog (Hh) signaling, an evolutionarily highly conserved morphogenetic network that regulates multiple aspects of development in vertebrate and invertebrate alike. Sonic hedgehog (Shh) is expressed by the lung epithelium, and it is thought to activate signaling in what has been named the "sub-epithelial mesenchyme" [4] to initiate a cascade of gene expression. Shh(−/−) lungs are profoundly abnormal, failing to undergo normal branching morphogenesis [5]. Importantly, Shh(−/−) lungs are reported to be entirely devoid of ACTA2-expressing cells. This places Hh signaling at the top of a putative regulatory cascade that controls the commitment and differentiation of multipotential mesenchymal cell progenitors along the ACTA2$^{pos}$ cell lineages.

Hh signaling is initiated upon binding of secreted Hh ligands to a receptor, Patched1 (Ptch1). In the absence of Hh ligands, Ptch1 inhibits the signaling activity of Smoothened (Smo), a seven transmembrane protein that shares sequence homology with G-protein coupled receptors. Binding the ligand releases Ptch1-mediated repression of Smo, activating its function at the cell surface that leads to transcriptional induction of the Hh signaling cascade. In Drosophila, Hh signaling is mediated solely by the zinc finger containing transcription factor family cubitus interruptus, ci/Gli [6, 7]. In vertebrates, three Gli molecules, Gli1, Gli2, and Gli3 function downstream of Hh signaling. That Gli1 is a direct transcriptional target of Hh signaling is supported by the results of many studies. For example, ectopic Shh induces Gli1 expression [8–11] and in the absence of Shh, Gli1 is not expressed [12]. Thus, Hh activity is both necessary and sufficient for Gli1 transcription. Recently Ahn and Joyner [13] generated mice carrying a knockin allele of Gli1-cre$^{ERT2}$. Gli1-Cre$^{ERT2}$ is expressed exclusively in cells that have received positive Hh signaling and only in the presence of tamoxifen (Tam). In these mice, addition of Tam defines the time point at which Gli1-expressing cells are marked. Thereafter, the progeny of

such cells can be followed with GFP using ROSA$^{mTmG}$ reporter mice. Thus, Gli1-Cre$^{ERT2}$ represents an inducible, highly reliable tool in genetic fate-mapping strategy to identify Hh-responding cells and their descendents during the process of development and postnatally only in the presence of Tam.

In this work, we have used the ability of Gli1-Cre$^{ERT2}$ to permanently label progenitor cell populations that are recipients of Hh signaling during early embryonic and postnatal development of the murine lung. By cell lineage analysis, we show that the targets of Hh signaling in the early lung serve as progenitors to contribute to a number of mesodermally derived differentiated cell types. The Gli1-Cre$^{ERT2}$-tagged cells contribute to the IMF cell population and are found in the PBSM and PVSM layers as well as within the mesothelium. Most importantly, we demonstrate that Hh-tagged mesodermal cells in early embryonic lung (E10.5–E11.5) serve as progenitors to SCMFs. Gene array analysis of Gli1-cre$^{ERT2}$-tagged cells in early embryonic lungs revealed the involvement of multiple key signaling pathways as such progenitors underwent differentiation during two critical periods of lung development. Ectopic activation of one such pathway, wingless-type MMTV integration site family (WNT) signaling, by targeted genetic inactivation of Apc resulted in expansion of the SCMF progenitor cell population and subsequently lead to formation of multiple myofibroblast masses in the perinatal lungs. The present findings pave the way toward isolation and characterization of SCMF progenitors, an admittedly important cell type whose understanding may be key to elucidating the mechanisms of alveolar formation in normal lung development and failure in both neonatal and adult lung diseases such as BPD and COPD, respectively.

## MATERIALS AND METHODS

### Mouse Breeding and Genotyping

All animals were maintained and housed in pathogen-free conditions according to the protocol approved by The University of Southern California Institutional Animal Care and Use Committee (IACUC) (Los Angeles, CA). Gli1-cre$^{ERT2}$; ROSA$^{mTmG}$ mice were generated by breeding the Gli1-cre$^{ERT2}$ [13] and the ROSA$^{mTmG}$ mice [Gt(ROSA)26Sor$^{tm4(ACTB-tdTomato,-EGFP)Luo}$/J, The Jackson Laboratory, Bar Harbor, ME, http://www.jax.org] on 129S6/SvEvTac genetic background. The Gli1-cre$^{ERT2}$; ROSA$^{mTmG}$ mice were then bred with the Apc$^{flox/flox}$ to generate the Apc$^{Gli1}$ mice. Genotyping of the transgenic mice were determined by polymerase chain reaction (PCR) with genomic DNA isolated from mouse tails or embryo tissue. The forward (F) and reverse primers (R) for transgenic mouse genotyping are listed below: Gli1-cre$^{ERT2}$: (forward) 5′-TAA AGA TAT CTC ACG TAC TGA CGG TG-3′ and (reverse) 5′-TCT CTG ACC AGA GTC ATC CTT AGC-3′; Apc$^{flox/flox}$: (forward) 5′-GAGAAACCCTGTC TCGAAAAAA-3′ and (reverse) 5′-AGTGCTGTTTCTATGAGTCAAC-3′.

### Immunofluorescent Staining

Immunofluorescent staining was performed as previously described [14]. Primary antibodies used are: mouse anti-GFP (green fluorescent protein) (Santa Cruz Biotechnology Inc., Santa Cruz, CA, http://www.scbt.com), mouse anti-ACTA2 (Sigma), rabbit anti-ACTA2 (Abcam, MA, http://www.abcam.com), rabbit anti-PDGFα (Cell Signaling, Beverly, MA, http://

www.cellsignal.com). Nuclei were counterstained with DAPI (4′,6-diamidino-2-phenylindole). For quantitative analyses, multiple images ($n > 8$, each contains 300–600 cells) were used to count the ratio of labeled cells. Quantitative data are presented as average values $\pm$ SEM. Sections from at least three lungs were analyzed for each data point.

For oil red O staining, frozen sections of neonatal lungs (8 um) were air dried, washed with tap water, rinsed with 60% isopropanol, and then stained with freshly prepared oil red O solution for 15 minutes. The stained sections were rinsed with 60% isopropanol followed by distilled water and then preserved in VECTASHELD mounting medium with DAPI (to visualize nuclei).

### Tamoxifen Administration

Tam was administered by oral gavages. For cell fate of neonatal lungs, two doses of Tam were administered to neonates at postnatal day 5 and 6 (PN5 and PN6). For cell fate of embryonic lungs, timed-pregnant $Gli1\text{-}cre^{ERT2}$; $ROSA^{mTmG}$ females received two doses of Tam at embryonic day 10.5 and 11.5 (E10.5 and E11.5). Animals were sacrificed at E12.5 to determine the pattern of $Gli1\text{-}cre^{ERT2}$ labeled cells. For lineage-tracing from embryonic stage to postnatal stage, Tam-treated pregnant females were sacrificed, and the pups were extracted by cesarean section at around E18.5. The pups were cleaned, dried, and fed by a foster mother that had delivered her own pups within a 2 day period.

### Cell Isolation

$Gli1\text{-}cre^{ERT2}$; $ROSA^{mTmG}$ embryonic lungs at stage of E14.5 or E18.5 were dissected in HBSS (GIBCO24020-117). Lung lobes were cut into small pieces, treated in 0.25% Trypsin-EDTA (GIBCO25200-056) at 37°C for 10 minutes, and transferred to 3 ml of Dulbecco's modified Eagle's medium (DMEM)/F12 with 1 mg/ml DNase I (Roche10104159001), followed by repeated pipetting. After adding 20 ml of DMEM/F12 containing 10% fetal bovine serum (FBS), the mixture was pipetted up and down until tissue was completely dissociated. Dissociated cells were filtered through 100 $\mu$m and 40 $\mu$m cell strainers, centrifuged at 4°C at 1,250 rpm for 5 minutes and resuspended in DMEM/F12. GFP$^{pos}$ cells were isolated by cell sorting (BD FACSAria III). GFP$^{neg}$ cells from $ROSA^{mTmG}$ (cre$^{negative}$) lungs isolated under the same condition were used as blank control for cell sorting. Relative abundance of GFP$^{pos}$ cells between E14.5 and E18.5 was calculated by comparison of the number of GFP$^{pos}$ cells from each whole lung, collected by cell sorting. Data represent average of four ratios from four E14.5 and four E18.5 isolations. $p$ value was calculated by one-sample $t$ test (hypothetical mean is 1).

### Gene Expression Profiling

$Gli1\text{-}cre^{ERT2}$; $ROSA^{mTmG}$ mouse embryonic lungs, which received Tam at E10.5 and E11.5, were dissected at E14.5 and E18.5. GFP$^{pos}$ cells were sorted (BD FACSAria III) and isolated for RNA extraction. RNA was subjected to Whole Mouse Genome Oligo Microarrays (Agilent, Palo Alto, CA, http://www.agilent.com). Raw intensities were log2-transformed and quantile normalized (Partek Genomics Suite 6.6). We selected probe sets with absolute fold change greater than 2 and a false discovery rate (FDR) value less than 0.05. Genes with raw intensity less than 50 in both stages are not included.

Ingenuity Pathways Analysis software (Ingenuity Systems, Redwood city, CA, http://www.ingenuity.com/) was used to analyze functional relationships of differentially expressed genes.

### Realtime PCR

Expression of selected genes was quantified by Realtime PCR using a LightCycler with LightCycler Fast Start DNA Master SYBR Green I Kit (Roche Applied Sciences, IN, http://www.roche-applied-science.com) as previously described [15]. Relative ratio of a target gene transcript in GFP$^{pos}$ cells between E18.5 and E14.5 was calculated with the $\Delta\Delta$Ct method [14]. All primers for Realtime PCR were designed by using the program of Universal ProbeLibrary Assay Design Center from Roche Applied Sciences. Sequences of the primers are listed in Supporting Information Table ST1.

### Labeling of Hh Targets in Embryonic Lungs

To determine an optimal dose of Tam that would activate $Gli1\text{-}cre^{ERT2}$ in the embryonic lung cells receiving Hh signaling, without causing abortion of the fetus, we tested two strategies. First we delivered a single dose of 4 mg of Tam per 30 g of body weight by gavage to pregnant $Gli1\text{-}cre^{ERT2}$; $ROSA^{mTmG}$ mice at gestational day E10.5 and examined their embryos within 12, 18–20, and 24 hours of exposure. Figure 1 shows that within the first 12 hours of Tam exposure only a minority of cells of distinctly mesenchymal lineage (i.e., NKX2.1$^{neg}$, Fig. 1A) are GFP$^{pos}$. The number of GFP$^{pos}$ cells increased in the 18–20, and the 24 hour post-Tam embryonic lungs (Fig. 1B, 1C, respectively). In both the 18–20 and 24 hour windows, GFP$^{pos}$ cells were localized around the branching epithelium within a region that has been referred to as the sub-epithelial mesenchyme [4]. Scant GFP$^{pos}$ cells were localized close to or within the mesothelium of the lung (arrows). As an alternative to maximize the labeling potential of the $Gli1\text{-}cre^{ERT2}$ we also administered two doses of Tam, 24 hours apart, delivered between E10.5 and E11.5. This regimen significantly increased the number of GFP$^{pos}$ cells in E12.5 lungs (Fig. 1D–1F). Examination of multiple embryonic lung samples showed that GFP$^{pos}$ cells tagged on E10.5–E11.5 made up nearly 27% ($\pm$0.075) of the total (DAPI positive) mesenchymal cell population in E12.5 lungs. The majority of these cells were undifferentiated interstitial cells in which ACTA2 was undetectable (Fig. 1D–1F). There were also few GFP$^{pos}$ cells near or within the peribronchial smooth muscle or perivascular smooth muscle layers (only PBSM shown). Importantly, these were ACTA2$^{pos}$ (Fig. 1D–1F).

### Postnatal Fate of Early Embryonic Hh Targets

Tam remains active for approximately 30 hours [13, 16]. Therefore, we adopted the "two-dose" Tam strategy (described above) and used the observations on E12.5 lungs as baseline for comparison in lineage analyses of E10.5–E11.5-tagged cells with later stages of lung development in the remainder of this project. Lineage tracing of cells labeled in E10.5–E11.5 embryos to PN14 showed that GFP$^{pos}$ cells can be found as IMF and a very rare population of cells in the mesothelium. Immunohistohemistry for ACTA2 revealed that the majority (94.5% $\pm$ 5.9%) of the GFP$^{pos}$ IMFs had now
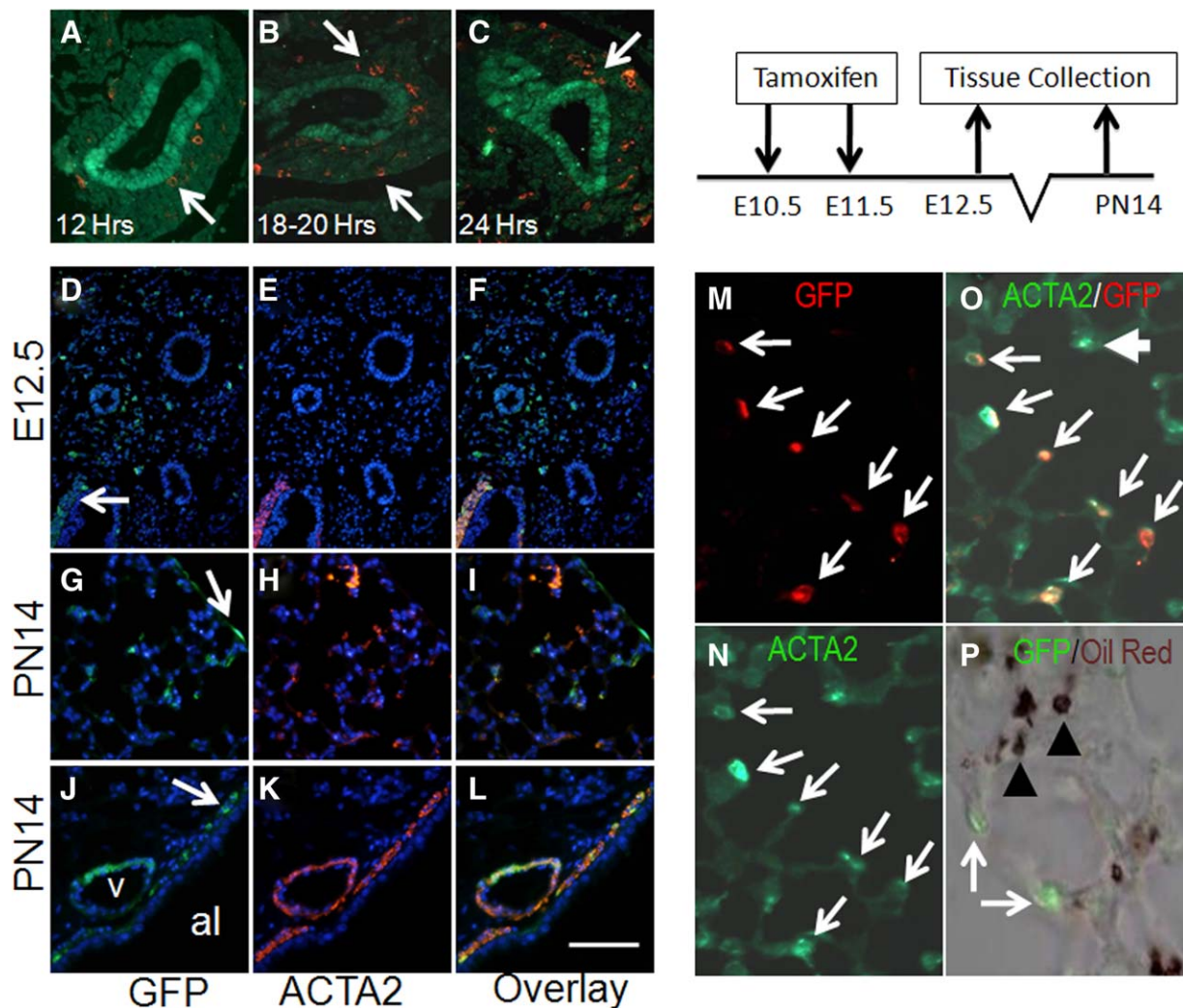
**Figure 1.** Lineage tracing of *Gli1-cre*$^{ERT2}$;ROSA$^{mTmG}$ labeled cells in embryonic lungs. **(A–C)**: Coimmunofluorescent staining of NKX2.1 (green) and GFP (red) in lungs of E11.5 *Gli1-cre*$^{ERT2}$;ROSA$^{mTmG}$ embryos, treated with one dose of Tam at E10.5. **(D–F)**: Coimmunofluorescent staining of GFP (green) and ACTA2 (red) in E12.5 lungs. **(G–L)**: Coimmunofluorescent staining of GFP (green) and ACTA2 (red) in PN14 *Gli1-cre*$^{ERT2}$;ROSA$^{mTmG}$ lungs. Arrows in panels (G) and (J) indicate GFP$^{pos}$ cells in mesothelial and peribronchial smooth muscle layer, respectively. **(M–O)**: Coimmunofluorescent staining of ACTA2 (green) and GFP (red) in secondary crest myofibroblast cells of PN14 pups that were treated with Tam at E10.5 and E11.5. **(P)**: Distribution of GFP (green) and oil red O (brown) are mutually exclusive in the Tam-treated PN14 lungs. Chart illustrates the experimental plan for panels (D–P). "v" indicates blood vessel. "al" indicates airway. Arrows indicate GFP$^{pos}$ cells. Arrowheads indicate oil red O positive staining. Scale bar = 85 $\mu$m for (D–F); 50 $\mu$m for (A–C), (G–L); 15 $\mu$m for (M–P). Abbreviations: ACTA2, alpha smooth muscle actin; GFP, green fluorescent protein; PN, postnatal.

differentiated to ACTA2$^{pos}$ (Fig. 1G–1I, 1M–1O). As expected, the GFP$^{pos}$ cells within the mesothelium showed no detectable expression of ACTA2 (arrow in Fig. 1G–1I). GFP$^{pos}$ cells were also found in the two structures composed of smooth muscle cells in PN14 lungs. Both PVSM and PBSM layers in PN14 lungs contained GFP$^{pos}$ cells (Fig. 1J–1L).

## Progenitors of SCMF are Committed in Early Lung Mesenchyme

We also examined the contribution of (Gli1$^{pos}$) GFP$^{pos}$ cells to the SCMFs. These are ACTA2$^{pos}$ cells appearing at the tip of the secondary crest found during the process of alveolization and thought to have a major role in this process. Unexpectedly, coimmunostaining with anti-GFP and anti-ACTA2 antibodies revealed that GFP$^{pos}$ cells labeled in E10.5–11.5 lungs or

their daughters also contributed to SCMFs, which appear only during alveolar formation. In PN14 *Gli1-cre*$^{ERT2}$;ROSA$^{mTmG}$ lungs, there were large number of GFP$^{pos}$ areas, within which upward of nearly 95% of the SCMFs were double positive for both GFP and ACTA2 (Fig. 1M–1O). Occasionally, ACTA2$^{pos}$ cells were observed that were not at first sight GFP$^{pos}$. However, careful examination showed that they were weakly stained with GFP antibody. Finally, due to spatial proximity to SCMFs we also examined whether any of the GFP$^{pos}$ cells identified in PN14 lungs were lipofibroblasts. Using oil red O, it is clear that GFP$^{pos}$ and oil-red-O$^{pos}$ cells are indeed distinct (Fig. 1P). This evidence shows that the SCMF cell fate is already established in E10.5–E11.5 embryonic lungs, a surprisingly early commitment for cells whose functional role is required during late and postnatal lung development.
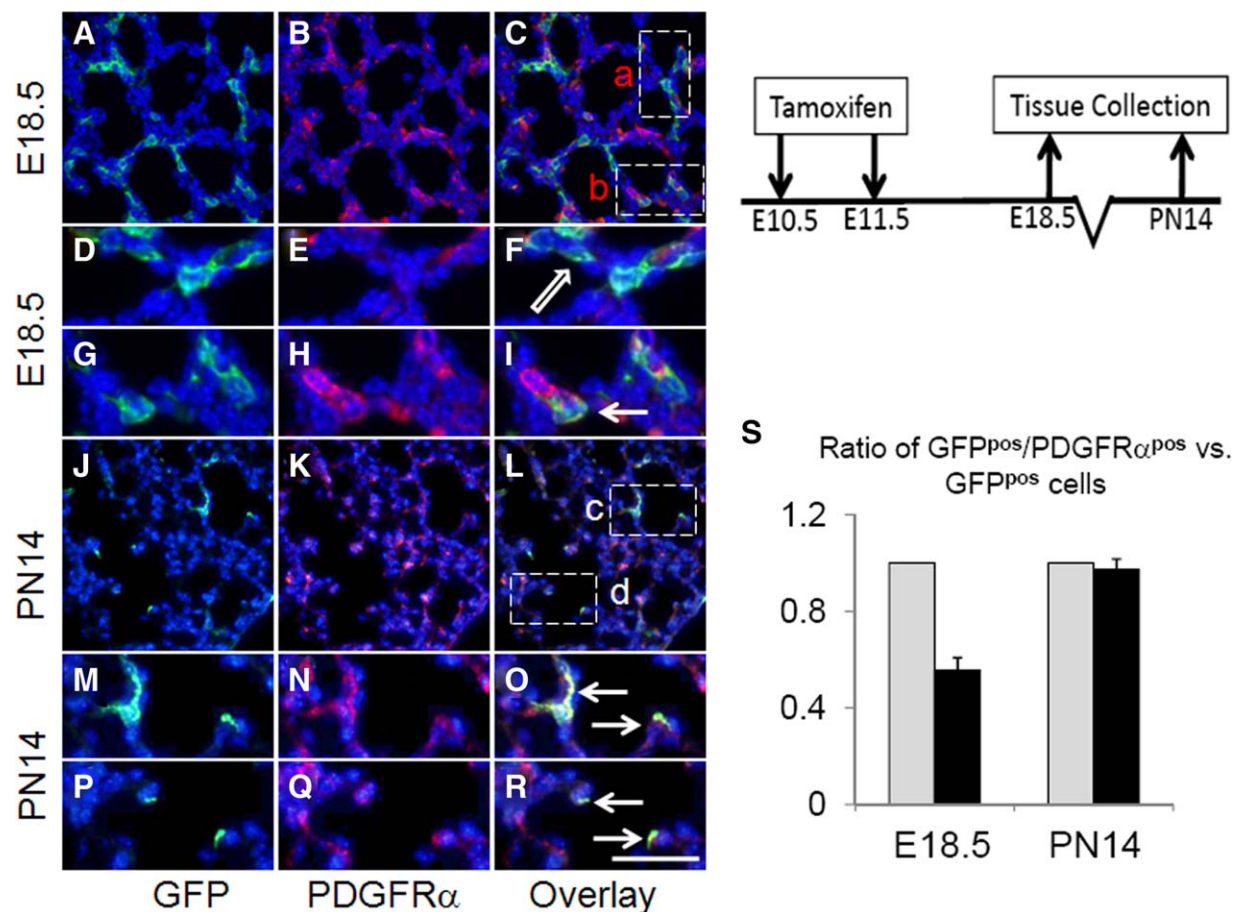
**Figure 2.** Timed pregnant females were treated with two doses of Tam at E10.5 and E11.5. *Gli1-cre^ERT2*;ROSA^mTmG^ lungs of E18.5 embryos and PN14 pups were collected and analyzed by coimmunofluorescent staining of GFP (green) and PDGFRα (red). **(D–F)**: Higher magnification of boxed area "a" rotated counterclockwise. **(G–I)**: Higher magnification of boxed area "b." **(M–O, P–R)**: Higher magnification of boxed areas "c", "d," respectively. Arrows indicate GFP**pos**/PDGFRα**pos** cells. Block arrows indicate GFP**pos**/PDGFRα**neg** cells. **(S)**: Calculated ratios of GFP**pos**/PDGFRα**pos** cells versus GFP**pos** cells (black bar). Total GFP**pos** cells were arbitrarily set as 100% (grey bar). Scale bar = 50 μm for (A–C), (J–L); 20 μm for (D–I), (M–R). Abbreviations: GFP, green fluorescent protein; PN, postnatal; PDGFR, platelet-derived growth factor receptor.

### *Gli1-cre^ERT2* Labeled Myofibroblast Progenitors Progressively Commit to PDGFRα Expression

PDGFRα has been proposed as an early marker of smooth muscle and myofibroblast cell lineages [1, 2]. In *PdgfA(−/−)* lungs, parenchymal and scattered cells expressing PDGFA's sole receptor, PDGFRα were absent, but expression in PBSM and PVSM appeared normal [1]. Correspondingly, myofibroblast cell differentiation and alveolization in *PdgfA(−/−)* lungs were blocked. To ascertain the temporal relationship between Hh signaling as assessed by GFP**pos** status and PDGFRα expression, we examined the lungs of embryos and newborns from *Gli1-cre^ERT2*;ROSA**mTmG** pregnant mice that received Tam on E10.5–E11.5. In E18.5, during the saccular stage of lung development, approximately 60% overlap was observed between GFP**pos** cells and those identified by immunostaining as PDGFRα**pos** (Fig. 2A–2I). In contrast, as the lungs developed to PN14 (alveolar stage) when extensive overlap between ACTA2**pos** and GFP**pos** cells was clearly evident (Fig. 1) nearly all (97.2% ± 4.4%) GFP**pos** cells were also PDGFRα**pos** by immunostaining (Fig. 2J–2R). The increase in GFP/PDGFRα double positive cells is unlikely caused by different proliferation rate of PDGFRα**pos** and PDGFRα**neg** cells, because it was reported that PDGFRα**pos** cells show decreased proliferation as

compared to PDGFRα**neg** lung fibroblast [17]. Thus, there is progressive acquisition of PDGFRα expression by E10.5–E11.5 mesenchymal targets of Hh signaling as lung development proceeds. These data demonstrate that activation of *Pdgfrα* expression occurs subsequent to commitment of the progenitor cells to ACTA2**pos** lineage.

### Hh Signaling Targets in Postnatal Lung

Hh signaling in the postnatal period of lung development has not been adequately studied. Therefore, we also examined the fate of cells receiving Hh signaling during the first week of life, a period during which alveolar formation is initiated. Newborn mice were treated with two doses of Tam on PN5 and PN6, and lungs were examined at two subsequent time points. Within a short window of only 5 days (PN11) subsequent to Tam administration, GFP**pos** cells appeared in four compartments including PBSM and PVSM layers (Fig. 3D–3I). Rare but definitively GFP**pos** cells were also found in the mesothelium of PN11 lungs (Fig. 3A–3C). The GFP**pos** cells in the PBSM and PVSM compartments were ACTA2**pos** (Fig. 3D–3I). In addition, SCMFs were uniformly GFP**pos** indicating that they were recipients of Hh signaling in early postnatal lung development. The source of the Hh ligand at this time period
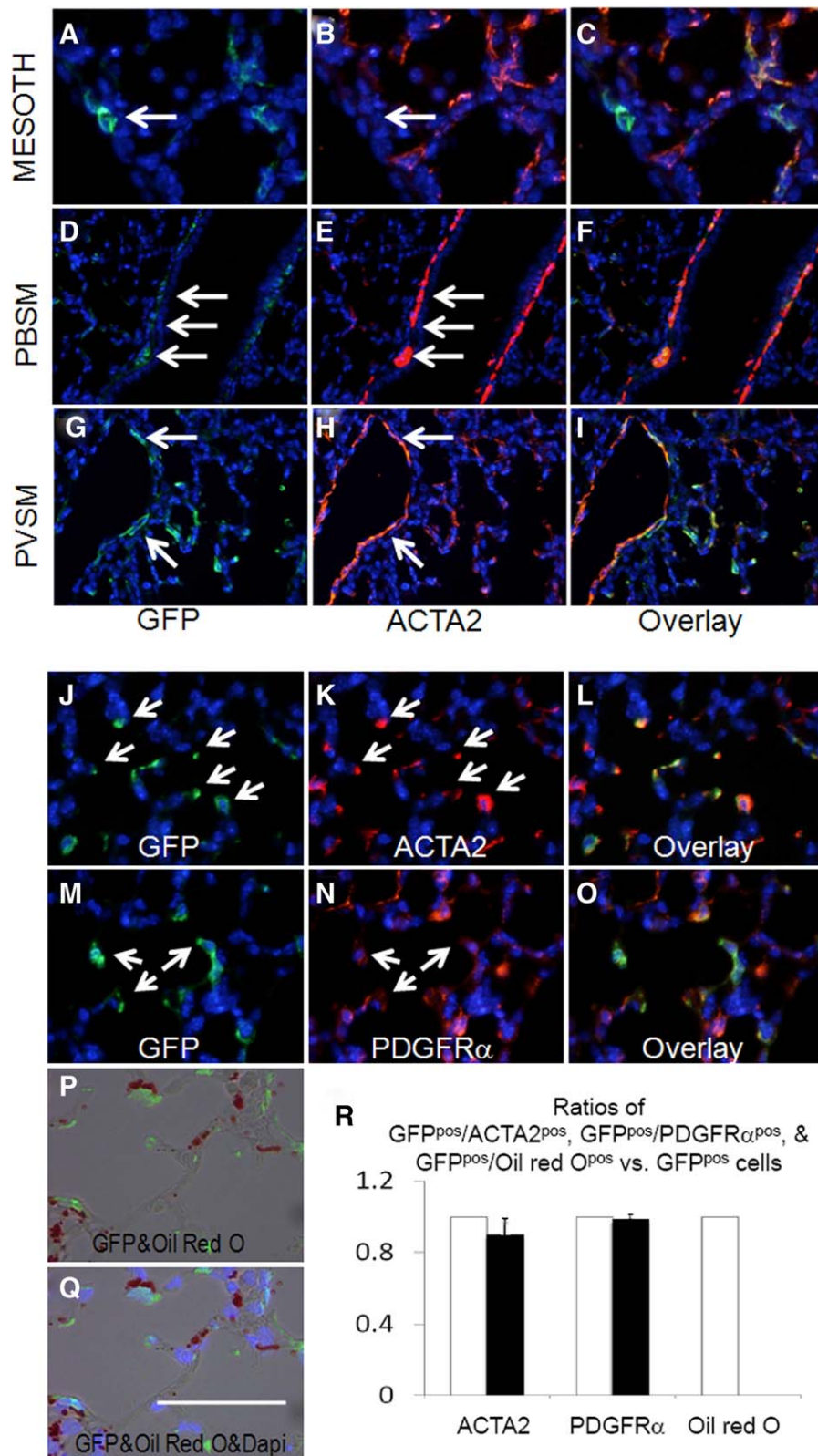
**Figure 3.** Distribution of GFP^{pos} cells in PN11 lungs treated with Tam on PN5 and PN6. **(A–L)**: Coimmunofluorescent staining of GFP (green) and ACTA2 (red) in areas around mesothelium (A–C), epithelial airways (D–F), blood vessels (G–I), and alveoli (J–L). **(M–O)**: Coimmunofluorescent staining of GFP (green) and PDGFRα (red) in alveolar interstitium. **(P, Q)**: Distribution of GFP and oil red O in the Tam-treated PN11 lungs. **(R)**: Ratios of GFP[pos]/ACTA2^{pos}, GFP[pos]/PDGFRα[pos], and GFP[pos]/oil-red-O^{pos} cells in total GFP^{pos} cells. Black bars represent the ratio of double positive cells. Total GFP^{pos} cells were arbitrarily set as 100% (white bars). Scale bar = 50 $\mu$m for (A–C), (J–Q); 100 $\mu$m for (D–I). Abbreviations: ACTA2, alpha smooth muscle actin; DAPI, 4′,6-diamidino-2-phenylindole; GFP, green fluorescent protein; PBSM, peribronchial smooth muscle fiber; PVSM, perivascular smooth muscle fiber; PDGFR, platelet-derived growth factor receptor.

in lung development remains unexplored [18]. GFP[pos] SCMFs were also uniformly ACTA2^{pos} and PDGFRα[pos] (Fig. 3J–3O, 3R). Importantly, as we found in Figure 3, none of the GFP[pos] SCMFs labeled on PN5–PN6 was positive for oil red O staining (Fig. 3P–3R).

Previous studies demonstrated that myofibroblasts are present specifically during alveolization and mostly disappear in normal adult lungs reflected as loss of ACTA2^{pos} expression [3]. This raised an interesting question regarding the fate of the GFP^{pos} cells labeled during PN5–PN6 period; whether the GFP^{pos} cells simply disappeared or survived but turned off *Acta2* expression? We therefore determined the fate of the cells labeled on PN5–PN6 after a prolonged period extending to 3 months of age. Here, GFP^{pos} cells or their progeny were found to survive within the PBSM (Fig. 4A–4C) and the PVSM (Fig. 4D–4F) layers. There were also rare GFP^{pos} cells in the mesothelial layer (Fig. 4G–4I). Importantly, only a few GFP^{pos} cells (less than 1% of total DAPI positive cells) were detected in the adult lung interstitium (Fig. 4J–4L). Whether these surviving GFP^{pos} cells are derived from a subpopulation of the IMF or other unidentified interstitial cells remains to be determined. Further characterization of the surviving GFP^{pos} cells revealed they express a number of differentiated mesodermal markers including Desmin, NG2, and PDGFR$\beta$ (Fig. 4M–4U). These have been shown to be expressed in "pericyte-like-cells" [19]. The GFP^{pos} cells also express tropoelastin (data not shown). However, expression of S100A4 (also known as FSP1 [19]) was not detected. Thus mesenchymal cells that are the target of Hh signaling on PN5–PN6 are found in multiple lung compartments with various differentiated mesenchymal phenotypes and survive to adulthood.

### Transcriptomic Analysis of Myofibroblast Cell Differentiation

Based mostly on histologic criteria, embryonic lung development has been divided into somewhat distinct periods [20]. Transition from the pseudoglandular stage that ends the process of branching morphogenesis (E14.5) to the canalicular/saccular stage (E18.5), which precedes alveolization (PN5–PN30) encompasses dramatic anatomical and cellular changes. Surprisingly, the molecular and genetic bases of this transition are poorly understood and represent a major challenge. In particular, multiple signaling pathways are thought to be involved in this transition [20]. The use of *Gli1-cre[ERT2]* presented an opportunity to label and therefore isolate a highly specific pool of mesodermal progenitors and examine the dynamics of gene expression in such cells as they underwent pseudoglandular to saccular transition. Accordingly, Hh-targeted mesodermal progenitors were tagged in *Gli1-cre[ERT2]*;*ROSA[mTmG]* lungs by two doses of Tam at E10.5–E11.5, and their GFP[pos] progeny were isolated from E14.5 and E18.5 lungs and purified by flow cytometry. The relative abundance of GFP^{pos} cells between E14.5 and E18.5 lungs is around 0.45 (±0.25, $p$ = .02). Gene expression profiles of purified GFP^{pos} cells were obtained on the Agilent gene array platform. The results were analyzed by comparative bioinformatics using the E14.5 versus E18.5 datasets. The microarray data were filtered for expression of various key functional categories of genes including levels of major signaling pathways. These analyses showed clear dynamic and profound changes (4,722 differentially expressed genes with >twofold change and FDR<0.05)

in genes belonging to all functional categories including transcription factors, signaling molecules, and extracellular matrix components (complete bioinformatic analysis of this study will be reported separately). In the signaling category, robust changes occurred in the WNT pathway whereby positive and negative regulators of the canonical WNT pathway were dynamically modulated (please see below and Table 1). Also, both transforming growth factor, beta (TGF$\beta$) and PDGFA/PDGFRα pathways which are critical for myofibroblast differentiation increased significantly as cells transitioned from the pseudoglandular to the cannalicular/saccular phases of lung development. Thus, transition of Hh-targeted cells tagged in E10.5–E11.5 from the pseudoglandular to cannalicular/saccular phase of lung development, a period of major changes that has remained little understood is accompanied by robust modulation of many components of various signaling pathways, among which there are extensive functional interactions or crosstalk (Supporting Information Fig. SF1). We propose that it is the total sum of the interactions among these signaling engines that ultimately controls the profound anatomical, cellular, and molecular changes that occur during this critical period of embryonic lung development.

### Ectopic Activation of Canonical WNT Signaling in Myofibroblast Progenitors by Apc Inactivation

A major finding of the transcriptomic analysis revealed alterations in a number of mediators of the WNT pathway with an overall decrease in canonical WNT activity as Hh-targeted mesodermal progenitors underwent transition from the pseudoglandular to the saccular phase of lung development (Table 1). For example, the canonical WNT signaling target CCND1 was significantly reduced (8.7-fold decrease, $p$ = 1.04E-06). In contrast, inhibitors of the canonical WNT signaling were highly increased. These included WNT5a (increased 7.6-fold, $p$ = 2.77E-06), WIF (increased 23.8-fold, $p$ = 6.72E-05), DKK3 (increased 6.8-fold, $p$ = 1.03E-05), and TLE1 (increased 2.0-fold $p$ = 5.8E-04). These changes were validated by Realtime PCR (Supporting Information Table ST2). To determine the functional significance of decreased WNT signaling specifically in the Hh-targeted progenitors, we used *Gli1-cre[ERT2]* and induced ectopic activation of WNT signaling by inactivating *Apc*, which encodes a component of the destructive complex for CTNNB1. Inactivation of *Apc* by Tam at E10.5 and E11.5 lead to increased canonical WNT activity represented by accumulation of CTNNB1 (Fig. 5) and increased LEF1 and AXIN2 expression (Supporting Information Fig. SF2). As a consequence, there was significant expansion of the mesodermal progenitor pools leading to formation of GFP[pos] focal masses, scattered within the lung parenchyma (Supporting Information Fig. SF3). At E14.5, the expanded progenitor pools with accumulated CTNNB1 were PDGFRα[neg] and expressed no detectable ACTA2, indicating they remain as early progenitors of IMF (Fig. 5). Proliferation of these cells is reduced as compared to the control lungs (Supporting Information Fig. SF2). Intriguingly, as the *Gli1-cre[ERT2]*;Apc[flox/flox] (*Apc[Gli1]*) lungs underwent further morphogenesis to E18.5, the expanded progenitor cells differentiated to a myofibroblast phenotype displaying robust expression of PDGFRα ACTA2, and fibronectin and eventually appearing as fibroblastic foci in the perinatal lungs (Fig. 5).
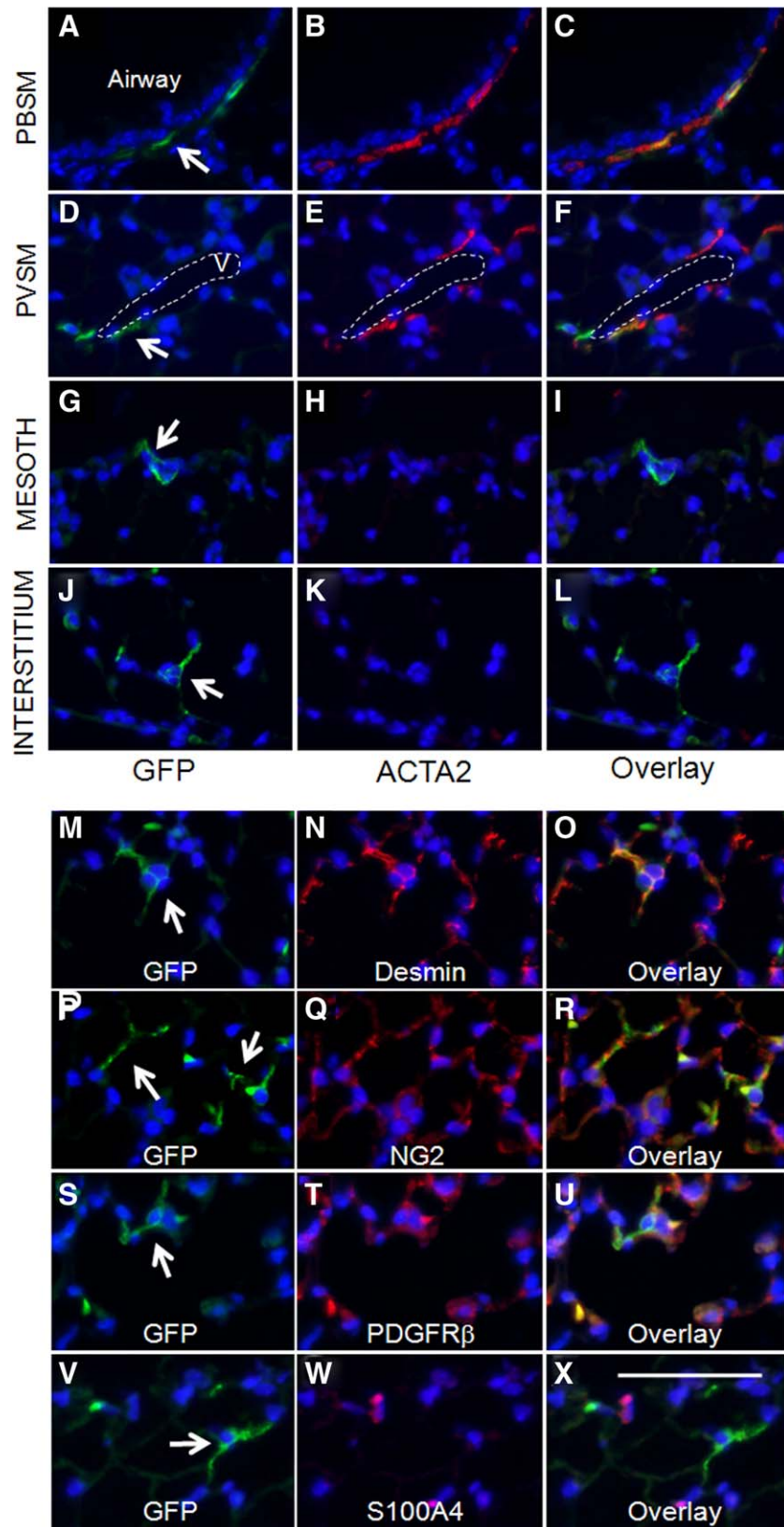
**Figure 4.** Distribution of GFP^{pos} cells in lungs of 3 month-old mice treated with Tam on PN5 and PN6. **(A–L)**: Coimmunofluorescent staining of GFP (green) and ACTA2 (red) in the areas around epithelial airways (A–C), blood vessels (D–F), mesothelium (G–I), and interstitium (J–L). Only small numbers of GFP^{pos} cells were present in alveolar interstitium. These cells were analyzed by coimmunofluorescent staining of GFP (green) and Desmin (red) **(M–O)**. GFP (green) and NG2 (red) **(P–R)**, GFP (green) and PDGFR$\beta$ (red) **(S–U)**, and GFP (green) and S100A4 (red) **(V–X)**. Arrows indicate GFP^{pos} cells. "v" indicates blood vessel. Scale bar = 50 $\mu$m. Abbreviations: ACTA2, alpha smooth muscle actin; GFP, green fluorescent protein; NG2, chondroitin sulfate proteoglycan 4; PDGFR, platelet-derived growth factor receptor; PBSM, peribronchial smooth muscle fibre; PVSM, perivascular smooth muscle fibre.

**Table 1.** Differentially expressed genes (E18.5 vs. E14.5 *Gli1-cre^ERT2*;ROSA^*mTmG*^ labeled cells) related to signaling pathways of PDGF, Wnt, TGF$\beta$, EGF, IGF, Shh, and FGF

| Genes with decreased expression in E18.5 | Genes with increased expression in E18.5 |
| --- | --- |
| PDGFsignaling (14 genes) | |
| SRF(serum response factor) | FOS(FBJ) murine osteosarcoma viral encogene homolog |
| ACP1(acid phosphatase1) | JUN(jun proto-oncogene) |
| MYC(V-myc avian myelocytomatosis viral oncogene homolog) | SPHK1(sphincosine kinase1) |
| PIK3R3(phosphoinositidde-3-kinase) | PIK3R1(phosphoinositide-3-Kinase, regulatory subunit3(gamma) |
| | PDGFRA(platelet-denvec growth factor,alpha polypeptide) |
| | INPP5K(inositol polyphosphate-5-phosphatase K) |
| | STAT3(signal transducer and activator of transcnption3) |
| | PRKCA(protein kinase C, alpha) |
| | RRAS(related RAS viral(r-ras) oncogene homolog) |
| | RRAS2(related RAS viral(r-ras) oncogene homolo(2) |
| Wnt/beta -catenin signaling (16 genes) | |
| CCND1(cyclin D1) | WIFK(WNT inhibitory factor 1) |
| MYC(V-myc avian myelocytomatosis viral oncogene homolog) | DKK3(dickkopf WNT signaling pathway inhibitor 3) |
| RSP02 [Mus musculus R-spondin 2 homolog) | WNT5A(wingless-type MMTV integration site family, member5A) |
| SFRP2(secreted frizzled-related protein2) | WNT5B(wingless-type MMTV integration site family, member 58) |
| CDH2(cadherin 2) | TLE1(transducin-like enhancer of split 1) |
| RUVBl2(RivB-like AAA ATPase 2) | lLK(integrin-linked kinase) |
| | JUN(jun proto-oncogene) |
| | LRP1(low density lipoprotein receptor-related protein 1) |
| | APPL2(adaptor protein, phsphotyrosine interation, PH domain and leucine zipper container2) |
| | FZD4(frizzled family receptor 4) |
| TGFbeta signaling (12 genes) | |
| MAP2K6(mitogen-activatec protein kinase kinase 6) | TGFB1(transformmg growth factor, beta1) |
| MAPK11 (mitogen-activated protein kinase 11) | BMP4(bone morphogenetic protein 4) |
| | TGFBR2(transforming growth factor, beta receptor II) |
| | TGFBR3(transforming growth factor, beta receptor III) |
| | JUN(jun proto-oncogene) |
| | FOS(FBJ murine osteosarcoma viral oncogene homolog |
| | INHA(inhibin, alpha) |
| | RRAS(related RAS viral(r-ras) oncogene homolog) |
| | PMEPA1(prostate transmembrare protein, androgen induced 1) |
| | RRAS2(related RAS viral(r-ras) oncogene homolog2) |
| EGF signaling (9 genes) | |
| SRF(serum response factor) | FOS(FBJ murine osteosarcoma viral oncogene homolog |
| MAPK11(mitogen-activated protein kinase 11) | JUN(jun proto-orcogene) |
| PIK3R3(phosphoinositidde-3-kinase) | PIK3Rl(phosphoinositide-3-kinase, reculatory subunit3(gamma) |
| | PRKCA(protein kinase C, alpha) |
| | STAT3(signal transducer and activator of transcription 3) |
| | ITPR2(inositol, 1,4.5-trisphosphate receptor, type2) |
| IGF siqnalinq (17 genes) | |
| SRF(serum response factor) | *CYR61(cysteine-rich, angiogenic inducer, 61)* |
| PRKAR2B(protein kinase,cAMP-dependent, regulatory, type II, beta) | FOS(FBJ murine osttosarcoma viral oncogene homolog |
| PIK3R3(phosphoinsitidee-3-kinase) | IGFBP3(insulin-like growth factor binding protein 3) |
| | IGF8P6(insulin-like growth factor binding protein 6) |
| | JUN(jun proto-oncogene) |
| | PIK3R1(prosphoinositide-3-kinase, regulatory subunit3(gamma) |
| | SOCS2(suppressor of cytokine signaling 2) |
| | STAT3(signal transducer and activator of transcription3) |
| | RRAS(related RAS viral(r-ras) oncogene homolog) |
| | IRS2(insulin receptor substrate 2) |
| | ICF1(insulin-li ke growth factor1,somatomedin C) |
| | CTGF(connective tissue growth factor) |
| | RRAS2(related RAS viral(r-ras) oncogene homolog2) |
| | FOXO1(forkhead box 01) |
| Sonic Hedgehog signaling (3 genes) | |
| PRKAR2B(protein kinase, cAMP-dependent, type II, beta) | HHIP(hecgehog interacting protein) |
| | PRKAG2(protein kinase, AMP-activated, gamma 2 non-catalytic subunit) |
| FGF signaling(12 genes) | |
| MAP2K6(mitgoen-activated protein kinase kinase6) | FGF7(fibroblast growth factor 7) |
| MAPK11(mitgoen-activated protein kinase 11) | FGFR4(fibroblast growth factor receptor 4) |
| PIK3R3(phosphoinositidde-3-kinase) | PIK3R1(phosphoinositide-3-Kinase, regulatory subunit3(gamma) |
| MAP3K5(mitogen-activated protein) | FGFR3(fibroblast growth factor receptor 3) |
| | STAT3(signal transducer and activator of transcription 3) |
| | FGF18(fibroblast growth factor 18) |
| | PRKCA(protein kinase C, alpha) |
| | Creb5(cAMP responsive ellement binding protein 5) |

Transcriptomic analyses of *Gli1-cre^ERT2*;ROSA^*mTmG*^ labeled cells were conducted with Whole Mouse Genome Oligo Microarrays (Agilent) and IPA software. Differentially expressed genes (identified by IPA with greater than twofold changes and an FDR value less than 0.05) are listed. The left column shows genes of each signaling pathway that decrease from E14.5 to E18.5. The right column shows genes of each signaling pathway that increase from E14.5 to E18.5.

Abbreviations: EGF, epidermal growth factor; FGF, fibroblast growth factor; IGF, insulin-like growth factor; PDGF, platelet-derived growth factor; TGF, transforming growth factor; Wnt, wingless-type MMTV integration site family; Shh, Sonic Hedgehog.
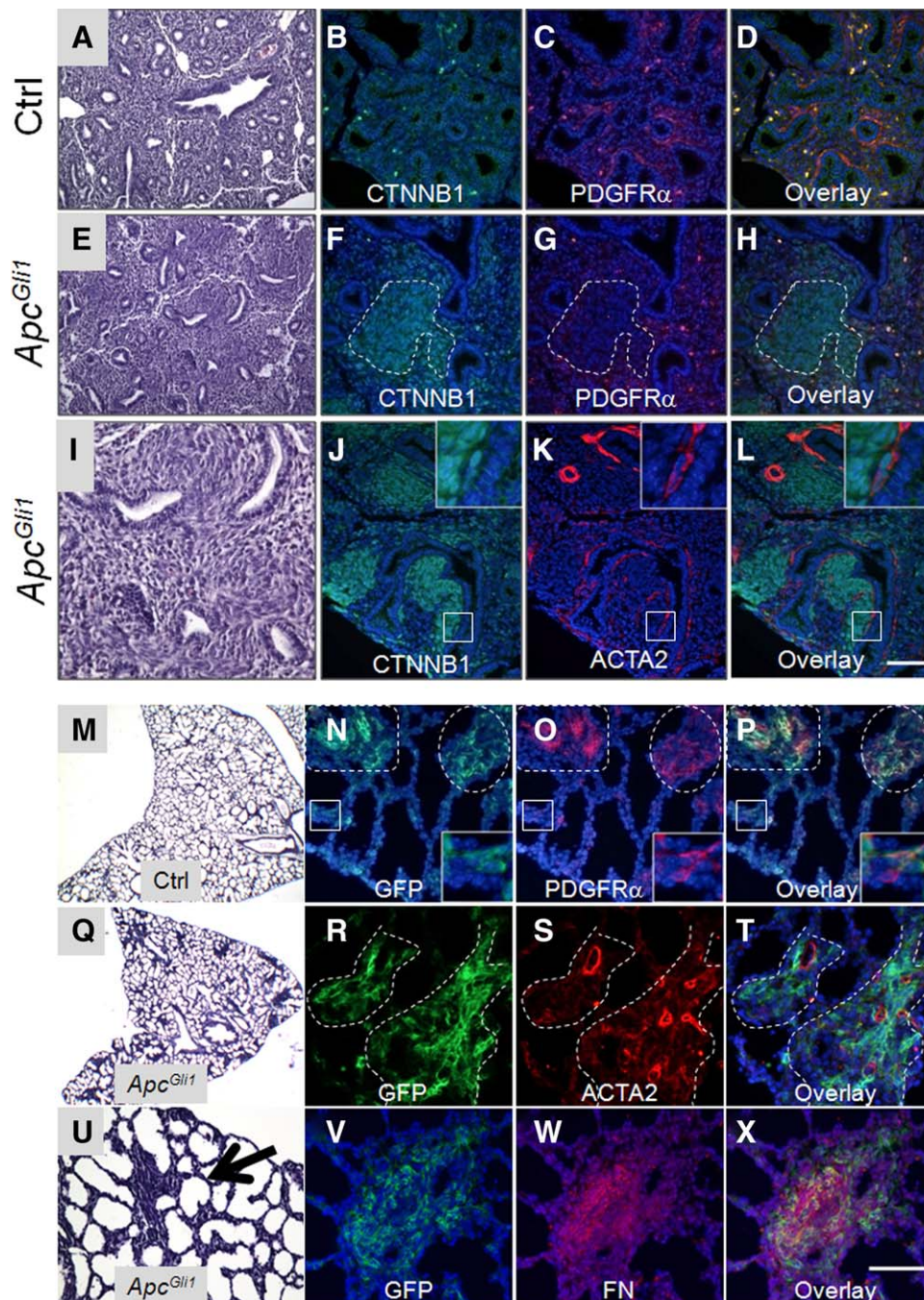
**Figure 5.** The $Gli1$-$cre^{ERT2}$;$Apc^{flox/flox}$ ($Apc^{Gli1}$) mice were treated with Tam at E10.5 and E11.5, and the lungs were characterized at E14.5 **(A–L)** and E18.5 **(M–X)**. (A, E, I): H&E staining of E14.5 control (A) and $Apc^{Gli1}$ (E, I) lungs. (B–D, F–H): Coimmunofluorescent staining of CTNNB1 (green) and PDGFRα (red) in E14.5 control (B–D) and $Apc^{Gli1}$ (F–H) lungs. (J–L): Coimmunofluorescent staining of CTNNB1 (green) and ACTA2 (red) in E14.5 $Apc^{Gli1}$ lungs. Inset shows higher magnification of boxed area, which contains peribronchial smooth muscle fiber (PBSM) with accumulated CTNNB1. (M, Q): H&E staining of E18.5 control (M) and $Apc^{Gli1}$ (Q) lungs. (U): Higher magnification of $Apc^{Gli1}$ lungs. Arrow indicates the area with formation of myofibroblast colonies. (N–P, R–T, V–X): Coimmunofluorescent staining of GFP and PDGFRα, GFP and ACTA2, GFP and FN in E18.5 $ROSA^{mTmG}$;$Apc^{Gli1}$ lungs, respectively. Inset in (N–P) shows higher magnification of boxed area. Dotted lines in (N–P) and (R–T) indicate myofibroblast colonies. Scale bar (L) = 50 μm for (B–D), (F–H), (J–L); 100 μm for (A), (E); 40 μm for (I). Scale bar (X) = 50 μm for (N–P), (R–T), (V–X); 150 μm for (M), (Q); 90 um for (U). Abbreviations: ACTA2, alpha smooth muscle actin; FN, fibronectin; GFP, green fluorescent protein; PDGFR, platelet-derived growth factor receptor.

## DISCUSSION

Cross-communication between the epithelium and its mesenchymal counterpart, a requirement in development of the lung and differentiation of its highly specialized cell types is predicated on key signaling pathways including fibroblast growth factor 10 (FGF10), bone morphogenetic protein 4 (BMP4), TGFβ, Wnt, and Hh. Shh is produced by the lung epithelium early in its morphogenesis and imparts specific
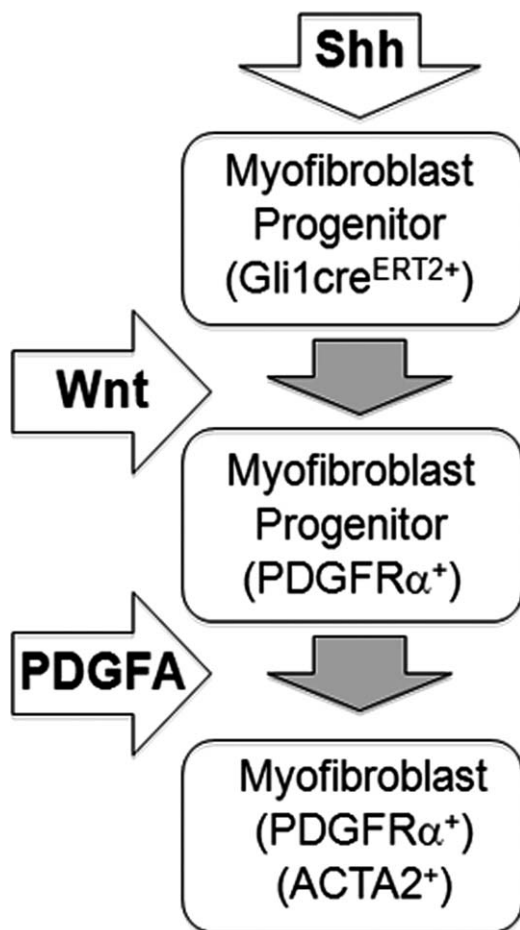
**Figure 6.** A simplified model illustrating the roles of Shh and Wnt signaling in alveolar myofibroblast differentiation. Shh signaling is activated in early myofibroblast progenitors, which express *Gli1-cre*[ERT2]. During myofibroblast differentiation, Wnt signaling controls the size of the progenitor pool. During saccular stage of lung development, PDGFA signaling is thought to be required for migration and distribution of myofibroblast progenitors to the lung interstitium to facilitate secondary crest formation, a key step in alveogenesis. Differentiated myofibroblasts localize to the tip of secondary crests and areas of the primary septa and express ACTA2 and PDGFRα. Abbreviations: PDGFA, platelet-derived growth factor-A; Shh, Sonic Hedgehog; Wnt, wingless-type MMTV integration site family.

instructional cues to the developing mesenchyme which in turn directs epithelial morphogenesis. *Shh(−/−)* lungs are profoundly abnormal in structure and are reported to lack the entire lineage of ACTA2^{pos} cells indicating absolute requirement of Hh signaling in either commitment or differentiation of these cell lineages.

The ACTA2^{pos} cell lineage comprises the fused smooth muscle cells of the PBSM and PVSM, and the scattered single cell IMF, the source of SCMF. While starting in early embryonic development, PBSM and PVSM are for the large part ACTA2^{pos}, IMFs become ACTA2^{pos} only in late embryonic or postnatal lung development and get lost in adult lungs. Owing to lack of specific markers, little is known regarding the lineage of IMFs. This study demonstrates that *Gli1-cre*[ERT2] represents a useful in vivo genetic tool to label, trace, and target IMF. Even though some PBSM and PVSM cells are also labeled by Gli1-cre[ERT2], these cells are easily distinguishable in the embryonic stage from IMF

progenitors based on their anatomic location and gene expression (i.e., ACTA2). Accordingly, we used *Gli1-cre*[ERT2] mice to first identify and then lineage trace Hh signaling targets during embryonic and postnatal lung development. Identification of Hh targets was based on GFP expression resulting from activation of *Gli1* in *Gli1-cre*[ERT2];ROSA[mTmG] lungs by two doses of Tam, 24 hours apart. This was done either during early embryonic development at E10.5–E11.5 or during postnatal lung development on PN5–PN6. Given the approximate 30 hour duration of Tam activity, we used the observations on E12.5 as baseline.

The majority of cells labeled by *Gli1-cre*[ERT2] in E10.5–E11.5 embryonic lungs were localized to the subepithelial mesoderm (Fig. 1). Shh is expressed by the pseudoglandular distal epithelium and acts on the adjacent subepithelial mesenchyme [21]. Consistent with the known range of Hh signaling, this implies that only the mesenchyme immediately proximal to the branching epithelium receives signaling. However, we also found GFP^{pos} cells distantly localized in the submesothelium and also within the mesothelium (Fig. 1). Hh ligands are secreted proteins whose spatial range of activity can be expanded by moieties such as cholesterol on its carboxyl terminus. Hh signaling is also dependent on proteoglycans and heparan sulfate synthesis by the target cells (on the range of hedgehog signaling). We cannot rule out the possibility of cell migration as the basis for the distantly localized GFP^{pos} cells.

Because SCMFs appear specifically at the alveolar stage, it is obvious that E10.5–E11.5, *Gli1-cre*[ERT2]- labeled IMFs serve as their progenitors. In contrast, whether cells tagged in E10.5–E11.5 lungs serve as progenitors to GFP[pos]/ACTA2^{pos} cells localized to the PBSM or PVSM of E12.5 lungs remains questionable. ACTA2^{pos} cells are found around the bifurcation of mainstem bronchi as early as E11.5 [22]. Therefore, we cannot rule out the likely possibility that *Gli1-cre*[ERT2] targets a select group of differentiated PBSM cells, which remain Hh-responsive. Progenitors of PBSM are proposed to be derived at least partly from FGF10^{pos} cells in the submesothelial mesoderm [4]. These cells are thought to migrate along the branching airways in a distal to proximal direction and undergo differentiation to become ACTA2^{pos} in response to SHH [23]. The origin of PVSM of the intralobular blood vessels remains to be determined. Wnt2^{pos};Gli1^{pos};Isl1^{pos} cardiopulmonary mesoderm progenitors tagged at E8.5 have been shown to give rise to pulmonary PVSM, PBSM as well as cardiomyocytes [24]. In contrast to the progressive (or sequential) pattern of PBSM differentiation, SCMF progenitors differentiate to ACTA2^{pos} cells in a synchronous manner (Fig. 1). These progenitor cells, which are first identified as interstitially scattered Gli1^{pos} with no detectable expression of ACTA2 display PDGFRα in mid-canalicular development [2], but subsequently become ACTA2^{pos} in near unison in the postnatal lung (Figs. (1 and 2)). In sum, the evidence strongly supports a model that cells labeled by *Gli1-cre*[ERT2] in E10.5–E11.5 represent progenitors of IMFs, which subsequently undergo differentiation to SCMFs during alveolization. This conclusion is further supported by the transcriptomic analysis (please see below).

The finding that Hh signaling as early as E10.5 establishes the commitment of SCMFs, a key and the least understood cell type in the lung is an important advancement that will undoubtedly facilitate the study of alveolar formation.

Alveogenesis is the last phase of lung development during which functional units of gas exchange are generated. In humans, alveogenesis commences in utero, but the process continues postnatally. In mice, the postnatal period spanning PN5–PN30 marks the process of alveolar formation. During alveogenesis, secondary septa subdivide the saccular space, thereby significantly expanding the gas exchange area. Septation requires elastic fibers deposited in the extracellular matrix by SCMFs whose identity and characteristics had hitherto remained poorly defined [20]. Topographically, SCMFs are localized to the alveolar septa. A major obstacle in characterization of SCMFs has been lack of technical ability to isolate them for detailed analysis. Lineage tracing of GFP<sup>pos</sup> cells tagged on E10.5–E11.5, a period of at least 7–10 days prior to the onset of alveogenesis clearly shows that this population harbors the progenitors of SCMFs (Fig. 1). Indeed we also found that SCMFs continue to receive Hh signaling during alveogenesis (Fig. 3). This result is consistent with the observation using *Gli1*<sup>nlacZ</sup> model by Liu et al. [18]. The source of Hh ligand in the postnatal lung remains unexplored.

Based on collective and currently available data, we propose a model (Fig. 6) in which Hh signaling is the key determinant of the multipotential mesenchymal cell commitment to the ACTA2<sup>pos</sup> lineage, as there is a purported lack of ACTA2<sup>pos</sup> cell types in *Shh(−/−)* lungs [5]. This decision point, regulated by Shh, is marked by activation of *Gli1* and using this information, we have now labeled and traced the progenitors and descendants of this lineage using the *Gli1-cre*<sup>ERT2</sup> mice [13]. Subsequent to Shh, PDGFA is key in regulating the decision that separates the fate of smooth muscle cells (PBSM and PVSM) from that of SCMFs. In *PdgfA(−/−)* lungs, SCMFs are absent and alveogenesis is blocked, while the PBSM and PVSM appear intact [1]. In these lungs, elastin is significantly diminished and expression of PDGFAs' sole receptor *Pdgfrα* on scattered IMFs, normally observed in wild type embryonic lungs is missing. Interestingly, PDGFRα<sup>pos</sup> cells and elastin fibers within the PBSM and PVSM are intact. This suggests that *Pdgfrα* activation occurs subsequent to Shh and Gli1 and in the smooth muscle lineage is independent of PDGFA. In contrast, *Pdgfrα* expression in progenitors of SCMF is dependent on PDGFA signaling. Thus, PDGFA is required for establishment of SCMF, but not PBSM or PVSM from a common Gli1<sup>pos</sup> progenitor cell population. Consistent with this model, reduction of PDGFRα does not significantly disrupt PBSM cells in E14.5 *Gli1-cre*<sup>ERT2</sup>;Apc<sup>flox/flox</sup> lungs (Fig. 5).

PDGFRα has been hitherto recognized as the earliest marker of SCMF progenitors [2]. Our findings demonstrate that Hh signaling precedes PDGFRα expression. In E18.5 lungs, we found only partial overlap between GFP<sup>pos</sup> and PDGFRα<sup>pos</sup> cells (Fig. 2). However, by P14, nearly all GFP<sup>pos</sup> cells had become both PDGFRα<sup>pos</sup> and ACTA2<sup>pos</sup> (Figs. 1 and 2). This observation was validated by the microarray analysis, which showed that *Pdgfrα* transcripts significantly increased (5.67-fold, $p < .005$) in the *Gli1-cre*<sup>ERT2</sup>-labeled cells transitioning from E14.5 to E18.5 phases of lung development.

Of note, in E18.5 *Gli1-cre*<sup>ERT2</sup>; ROSA<sup>mTmG</sup> lungs, a large portion (60.2% ± 9.8%) of PDGFRα<sup>pos</sup> cells are GFP<sup>neg</sup>. The origin and lineage of these cells remain unknown. One possibility is that not all SCMF progenitors are exposed to Shh signaling around E10.5 and E11.5. Another possibility is that not all

PDGFRα<sup>pos</sup> cells serve as SCMF progenitors, even though PDGF-A signaling is required for SCMF differentiation. In agreement with this possibility, Chen et al. [25] reported that during compensatory lung growth, only a subset of PDGFRα<sup>pos</sup> cells (the dim PDGFRα expressing cells) serve as myogenic precursors.

Smooth muscle differentiation is also dependent on canonical WNT (WNT/CTNNB1) signaling [26–28]. *Wnt7b* broadly regulates the development of smooth muscle [28]. In *Wnt7b (−/−)* mice, PVSM development is disrupted causing perinatal pulmonary hemorrhage [29]. *Wnt2* acts upstream of *Fgf10* and the critical transcription factors myocardin and Mrtf-B to regulate early smooth muscle cell differentiation [30]. The role of *Wnt2* or *Wnt7b* in SCMF has not been investigated. In this study, we found the role of canonical WNT signaling during IMF differentiation to be more complex. In early stages (i.e., E14.5), WNT appears to be critical for regulating the pool of IMF. Ectopic activation of WNT signaling lead to expansion of this progenitor pool, which resulted in perinatal appearance of mesodermal cellular masses. Therefore, reduced WNT signaling observed in the transcriptomic analysis (Table 1) is likely related to controlling the size of the IMF progenitor pool.

Disruption of a number of signaling pathways causes abnormal alveolar development. For example, insulin-like growth factor 1 (IGF1) deficiency in mice disrupts alveologenesis and leads to neonatal death [31]. Transcriptomic analysis in *Igf1(−/−)* lungs revealed reduced expression of two major genes; *Klf2* and *Egr1* suggesting their potential involvement [31]. Our microarray analysis showed increased transcripts for multiple mediators of IGF pathway during the transition of Hh-targeted wild type mesodermal cells from E14.5 to E18.5 (Table 1). *Klf2* increased by 17.29-fold ($p < .005$) and *Egr1* by 18.91-fold ($p < .005$) prior to the onset of alveogenesis. Of interest, treatment of *Igf1(−/−)* lungs with IGF1 increased distal lung maturation and expression of *Klf2* and *Cyr61*. Our array analysis also showed an 11.4-fold increase in Cyr61 ($p < .005$). Collectively, these findings support the assertion that the GFP<sup>pos</sup> cells tagged on E10.5–E11.5 represent a cell population with properties consistent with those of SCMFs and their role in alveologenesis.

The mechanisms that regulate late-stage myofibroblast differentiation may involve interactions of multiple pathways. For example, transcripts for several mediators of TGF$\beta$, IGF, and PDGF signaling are increased during the E14.5 → E18.5 transition (Table 1). The precise "signaling stoicheometry" between Wnt and TGF$\beta$, IGF and PDGF may be critical in achieving normal SCMF differentiation, which in turn is essential for alveogenesis. But ultimately the dynamics, and precisely "regulated" interactions among multiple signaling pathways appears necessary for proper differentiation of myofibroblast progenitors. In this study, alterations in a single signaling pathway, that of WNT alone in *Gli1-cre*<sup>ERT2</sup>;Apc<sup>flox/flox</sup> lungs caused a phenotype similar but not identical to the fibroblastic masses found in interstitial pulmonary fibrosis (IPF). Not identical, as the clinical IPF is a highly complex pathology that includes not only fibroblastic masses (as in *Gli1-cre*<sup>ERT2</sup>;Apc<sup>flox/flox</sup> lungs) but also epithelial malfunction [32, 33]. Increased canonical WNT signaling has been observed in human and experimental IPF, but it is usually combined with alterations in multiple other signaling pathways, such as TGF$\beta$, PDGF, and IGF [34, 35]. As the change

in WNT signaling via inactivation of *Apc* by *Gli1-cre*<sup>ERT2</sup> was induced at a specific time and only in a specific subpopulation of mesodermal cells, these findings raise the intriguing possibility that this population may be particularly sensitive to alterations in Wnt signaling and prone to contributing to mesenchymal masses like those found in IPF. Whether as such this cell population may contribute to and thus represent a new and potential therapeutic target in IPF remains a future challenge.

## CONCLUSIONS

Our studies demonstrate that progenitors of alveolar or secondary crest myofibroblasts are committed during early lung development. Differentiation of alveolar myofibroblast is regulated by interactions amongst multiple signaling pathways including PDGFA, TGFb and WNT. The Gli1-creERT2 mouse line represents a novel tool in studying the mechanism of myofibroblast cell differentiation and alveolar formation during lung development.

## AUTHOR CONTRIBUTIONS

C.L. and P.M.: conceived and designed the study; C.L., M.L., S.L., Y.X., C.Y.Y., and A.L.: performed the experiments and collected data; C.L. and P.M.: interpreted data; C.Li, P.M., Z.B., and S.D.L.: helped with interpretation of data and wrote the manuscript.

## DISCLOSURE OF POTENTIAL CONFLICTS OF INTEREST

The authors indicate that they have no potential conflict of interest.

## REFERENCES

1  Bostrom H, Willetts K, Pekny M et al. PDGF-A signaling is a critical event in lung alveolar myofibroblast development and alveogenesis. Cell 1996;85:863–873.

2  Lindahl P, Karlsson L, Hellstrom M et al. Alveogenesis failure in PDGF-A-deficient mice is coupled to lack of distal spreading of alveolar smooth muscle cell progenitors during lung development. Development 1997;124:3943–3953.

3  Yamada M, Kurihara H, Kinoshita K et al. Temporal expression of alpha-smooth muscle actin and drebrin in septal interstitial cells during alveolar maturation. J Histochem Cytochem 2005;53:735–744.

4  White AC, Xu J, Yin Y et al. FGF9 and SHH signaling coordinate lung growth and development through regulation of distinct mesenchymal domains. Development 2006;133:1507–1517.

5  Pepicelli CV, Lewis PM, McMahon AP. Sonic hedgehog regulates branching morphogenesis in the mammalian lung. Curr Biol 1998;8:1083–1086.

6  Bai CB, Stephen D, Joyner AL. All mouse ventral spinal cord patterning by hedgehog is Gli dependent and involves an activator function of Gli3. Dev Cell 2004;6:103–115.

7  Methot N, Basler K. An absolute requirement for Cubitus interruptus in Hedgehog signaling. Development 2001;128:733–742.

8  Marigo V, Johnson RL, Vortkamp A et al. Sonic hedgehog differentially regulates expression of GLI and GLI3 during limb development. Dev Biol 1996;180:273–283.

9  Grindley JC, Bellusci S, Perkins D et al. Evidence for the involvement of the Gli gene family in embryonic mouse lung development. Dev Biol 1997;188:337–348.

10  Hynes M, Stone DM, Dowd M et al. Control of cell pattern in the neural tube by the zinc finger transcription factor and oncogene Gli-1. Neuron 1997;19:15–26.

11  Lee J, Platt KA, Censullo P et al. Gli1 is a target of Sonic hedgehog that induces ventral neural tube development. Development 1997;124:2537–2552.

12  Bai CB, Auerbach W, Lee JS et al. Gli2, but not Gli1, is required for initial Shh signaling and ectopic activation of the Shh pathway. Development 2002;129:4753–4761.

13  Ahn S, Joyner AL. Dynamic changes in the response of cells to positive hedgehog signaling during mouse limb patterning. Cell 2004;118:505–516.

14  Li C, Li A, Li M et al. Stabilized β-catenin in lung epithelial cells changes cell fate and leads to tracheal and bronchial polyposis. Dev Biol 2009;334:97–108.

15  Li C, Hu L, Xiao J et al. Wnt5a regulates Shh and Fgf10 signaling during lung development. Dev Biol 2005;287:86–97.

16  Ahn S, Joyner AL. In vivo analysis of quiescent adult neural stem cells responding to Sonic hedgehog. Nature 2005;437:894–897.

17  McGowan SE, McCoy DM. Platelet-derived growth factor-A regulates lung fibroblast S-phase entry through p27(kip1) and FoxO3a. Respir Res 2013;14:68.

18  Liu L, Kugler MC, Loomis CA et al. Hedgehog signaling in neonatal and adult lung. Am J Respir Cell Mol Biol 2013;48:703–710.

19  Rock JR, Barkauskas CE, Cronce MJ et al. Multiple stromal populations contribute to pulmonary fibrosis without evidence for epithelial to mesenchymal transition. Proc Natl Acad Sci USA 2011;108:E1475–E1483.

20  Morrisey EE, Hogan BL. Preparing for the first breath: Genetic and cellular mechanisms in lung development. Dev Cell 2010;18:8–23.

21  Bellusci S, Furuta Y, Rush MG et al. Involvement of Sonic hedgehog (Shh) in mouse embryonic lung growth and morphogenesis. Development 1997;124:53–63.

22  Hines EA, Jones MK, Verheyden JM et al. Establishment of smooth muscle and cartilage juxtaposition in the developing mouse upper airways. Proc Natl Acad Sci USA 2013;110:19444–19449.

23  Mailleux AA, Kelly R, Veltmaat JM et al. Fgf10 expression identifies parabronchial smooth muscle cell progenitors and is required for their entry into the smooth muscle cell lineage. Development 2005;132:2157–2166.

24  Peng T, Tian Y, Boogerd CJ et al. Coordination of heart and lung co-development by a multipotent cardiopulmonary progenitor. Nature 2013;500:589–592.

25  Chen L, Acciani T, Le Cras T et al. Dynamic regulation of platelet-derived growth factor receptor alpha expression in alveolar fibroblasts during realveolarization. Am J Respir Cell Mol Biol 2012;47:517–527.

26  De Langhe SP, Sala FG, Del Moral PM et al. Dickkopf-1 (DKK1) reveals that fibronectin is a major target of Wnt signaling in branching morphogenesis of the mouse embryonic lung. Dev Biol 2005;277:316–331.

27  De Langhe SP, Carraro G, Tefft D et al. Formation and differentiation of multiple mesenchymal lineages during lung development is regulated by beta-catenin signaling. PLoS One 2008;3:e1516.

28  Cohen ED, Ihida-Stansbury K, Lu MM et al. Wnt signaling regulates smooth muscle precursor development in the mouse lung via a tenascin C/PDGFR pathway. J Clin Invest 2009;119:2538–2549.

29  Shu W, Jiang YQ, Lu MM et al. Wnt7b regulates mesenchymal proliferation and vascular development in the lung. Development 2002;129:4831–4842.

30  Goss AM, Tian Y, Cheng L et al. Wnt2 signaling is necessary and sufficient to activate the airway smooth muscle program in the lung by regulating myocardin/Mrtf-B and Fgf10 expression. Dev Biol 2011;356:541–552.

31  Pais RS, Moreno-Barriuso N, Hernandez-Porras I et al. Transcriptome analysis in prenatal IGF1-deficient mice identifies molecular pathways and target genes involved in distal

lung differentiation. PLoS One 2013;8: e83028.

**32** Selman M, Pardo A. Idiopathic pulmonary fibrosis: An epithelial/fibroblastic cross-talk disorder. Respir Res 2002;3:3.

**33** Li M, Krishnaveni MS, Li C et al. Epithelium-specific deletion of TGF-beta receptor type II protects mice from bleomycin-induced pulmonary fibrosis. J Clin Invest 2011;121: 277–287.

**34** Maeda A, Hiyama K, Yamakido H et al. Increased expression of platelet-derived growth factor A and insulin-like growth factor-I in BAL cells during the development of bleomycin-induced pulmonary fibrosis in mice. Chest 1996;109:780–786.

**35** Trojanowska M. Role of PDGF in fibrotic diseases and systemic sclerosis. Rheumatology (Oxford) 2008;47(suppl 5):v2–v4.

See www.StemCells.com for supporting information available online.